



HAL
open science

Non-radiative processes in protonated diazines, pyrimidine bases and an aromatic azine

Gustavo A. Pino, Géraldine Feraud, Michel Broquier, Gilles Grégoire, Satchin Soorkia, Claude Dedonder, Christophe Juvet

► **To cite this version:**

Gustavo A. Pino, Géraldine Feraud, Michel Broquier, Gilles Grégoire, Satchin Soorkia, et al.. Non-radiative processes in protonated diazines, pyrimidine bases and an aromatic azine. *Physical Chemistry Chemical Physics*, 2016, 10.1039/C6CP01345G . hal-01346414

HAL Id: hal-01346414

<https://hal.science/hal-01346414>

Submitted on 18 Jul 2016

HAL is a multi-disciplinary open access archive for the deposit and dissemination of scientific research documents, whether they are published or not. The documents may come from teaching and research institutions in France or abroad, or from public or private research centers.

L'archive ouverte pluridisciplinaire **HAL**, est destinée au dépôt et à la diffusion de documents scientifiques de niveau recherche, publiés ou non, émanant des établissements d'enseignement et de recherche français ou étrangers, des laboratoires publics ou privés.



Distributed under a Creative Commons Attribution - NonCommercial 4.0 International License

Non radiative processes in protonated aromatic azine, diazines and pyrimidine bases.

Gustavo A. Pino,¹ Géraldine Feraud,^{4†} Michel Broquier,^{2,3} Gilles Grégoire,^{2,3} Satchin Soorkia,^{2,3} Claude Dedonder,⁴ Christophe Jouvét⁴

1) Instituto de Investigaciones en Físico Química de Córdoba (INFIQC) CONICET – UNC. Dpto. de Fisicoquímica – Facultad de Ciencias Químicas – Centro Láser de Ciencias Moleculares – Universidad Nacional de Córdoba, Ciudad Universitaria, X5000HUA Córdoba, Argentina

2) Centre Laser de l'Université Paris-Sud (CLUPS/LUMAT), Univ. Paris-Sud, CNRS, IOGS, Université Paris-Saclay, F-91405 Orsay (France)

3) Institut des Sciences Moléculaires d'Orsay (ISMO), CNRS, Univ. Paris Sud, Université Paris-Saclay, F-91405 Orsay (France)

4) CNRS, Aix Marseille Université, PIIM UMR 7345, 13397, Marseille, France

† Present address: LERMA, Sorbonne Universités, UPMC Univ. Paris 06, Observatoire de Paris, PSL Research University, CNRS, F-75252, Paris, France

Abstract

The excited state lifetimes of DNA bases are often very short due to very efficient non-radiative processes assigned to the $\pi\pi^*$ - $n\pi^*$ coupling. A set of protonated aromatic diazine molecules (pyridazine, pyrimidine and pyrazine $C_4H_5N_2^+$) and protonated pyrimidine DNA bases (cytosine, uracil and thymine), as well as protonated pyridine ($C_5H_6N^+$), have been investigated. For all these molecules except one tautomer of protonated uracil (enol-keto), the electronic spectroscopy exhibits vibrational line broadening. Excited state geometry optimization at the CC2 level has been conducted to find out whether the excited state lifetimes measured from line broadening can be correlated to the calculated ordering of the $\pi\pi^*$ and $n\pi^*$ states and the $\pi\pi^*$ - $n\pi^*$ energy gap. The short lifetimes, observed when one nitrogen atom of the ring is not protonated, can be rationalized by relaxation of the $\pi\pi^*$ state to the $n\pi^*$ state or directly to the electronic ground state through ring puckering.

1. Introduction

DNA and RNA are fundamental molecules in nature, composed by only five nucleobases in specific tautomeric forms (canonical structures), two purine bases: adenine (A) and guanine (G) and three pyrimidine bases: uracil (U), thymine (T) and cytosine (C) that constitute the alphabet of the genetic code since the beginning of life on Earth. This is a prominent example of the constricted natural selection upon which life was developed. In understanding the prebiotic chemistry, one fundamental question to answer is how these molecules were chosen by nature in the early stages of Earth before the development of life?¹

Among the environmental selection pressures and evolutionary processes suggested to be operating in the selection of the building blocks of life, UV irradiation has been considered a prominent driver of prebiotic chemistry, and an important pressure for the most photo stable molecules. The ozone layer did not exist, 4×10^9 years ago, and then the Earth was exposed to very strong and energetic solar radiation that could be absorbed by many heterocyclic molecules present in the primordial soup. For this reason, it has been suggested that the excited state dynamics of these heterocycles has played a decisive role in the natural selection of the building blocks of the life, i.e. those with the highest photo stability and therefore with the maximum probability to remain unchanged over time have been selected.²

The excited state lifetime of several purine and pyrimidine derivatives including the DNA/RNA bases, have been determined either in solution or in the gas phase. For example, in pyridine and diazine, the first excited state is a $n\pi^*$ state with low oscillator strength and lifetimes in the picosecond domain obtained through fluorescence detection: 32 ps for pyridine,^{3,4} 120 ps for pyrazine,⁵ 320 ps for pyridazine,⁶ and around 2 ns for pyrimidine.⁷ When the excited state lifetimes get even shorter, multi photon ionization (MPI) or photoelectron imaging with femtosecond lasers is possible but these lasers are not easily scanned. This is demonstrated in the uracil case for which gas phase electronic spectra do not seem to exist. In pyridine and diazine, the $\pi\pi^*$ excited state that bears the oscillator strength has an ultra-short lifetime: 2.2 ps for pyridine in solution⁸ and 20 fs for gas phase pyrazine.^{9,10} Remarkably, the canonical DNA/RNA bases have the shortest excited state lifetimes. These studies have been recently reviewed.¹¹ The short excited state lifetime of the canonical DNA bases is associated with an ultrafast internal conversion (IC) to the ground state S_0 and it is assumed to be responsible for the remarkable photo stability of these molecules. However, the detailed mechanisms leading to IC are still under discussion.¹²

In the case of the pyrimidine bases, many theoretical works¹³⁻¹⁷ have been devoted to study the mechanism of internal conversion from the excited $\pi\pi^*$ toward either the $n\pi^*$ or the S_0 states. Many pathways are leading to the internal conversion, either indirectly from the $\pi\pi^*$ to the $n\pi^*$ and then to the S_0 state or directly from $\pi\pi^*$ to S_0 through out-of-plane deformations of the ring and/or amino group.

The deactivation pathways of these molecules as well as their excited state lifetimes are strongly affected by their structures, e.g. of all the tautomers of the DNA bases, those biologically relevant (canonical tautomers found in the DNA) have the shortest excited state lifetime minimizing the possibility of photochemical damage. In the case of the CG pair, only the structures assigned as Watson-Crick have broad spectra, corresponding to a very short excited state lifetime. Furthermore, chemical substitution in the canonical tautomers of the DNA bases strongly affects the excited state lifetime.

To get more insight into the factors that determine the photochemical properties of heterocyclic organic molecules that could be at the origin of the natural selection of the DNA bases, more systematic studies in the gas phase are needed. In this work, we have studied protonated aromatic diazines (DAz) since adding a proton on these molecules is a way to controllably change the bond structure of the aromatic ring and to change the character of the excited states, even leading to changes in the energy order between the $n\pi^*$ and the $\pi\pi^*$ states. This will give an exhaustive set of experimental data that can be used to validate ab-initio calculations. In addition, the protonation of nucleobases and its effect on their properties are of interest in prebiotic chemistry since early oceans may have displayed significant fluctuations in their pH values and thus protonated and deprotonated species are expected to be present at that time.

For protonated molecules in the gas phase, due to the small density of ions produced experimentally, fluorescence or absorption measurements are not favorable and the absorption is rather monitored through ion photo-fragmentation. The fragmentation mechanism is most effective when the non-radiative processes are very efficient i.e. when there is a very fast internal conversion, which results in a shortening of the excited state lifetime as compared to the radiative one. Another advantage to working with ions is that the photodissociation dynamics can be followed for many orders of magnitude from fs using lasers to seconds using ion storage rings or ion traps. Indeed, the reactive event can extend over more than 10 orders of magnitude in time as shown in the case of tryptophan,¹⁸ for which the excited state

dynamics occurs in the 10^{-13} s range and some fragmentations following the optical excitation are still observed after 10^{-2} s.

The electronic spectra of all protonated DNA/RNA bases have been recently published at low¹⁹ and room temperature.²⁰ Many tautomers, which can have very different excited state lifetimes, have been observed. For some tautomers, line broadening is observed which indicates a very short excited state lifetime of the locally excited state $\pi\pi^*$ (200/50 fs) according to the uncertainty principle. One should mention that a measurement of the excited state lifetime is linked to the dynamics of the initially excited $\pi\pi^*$ state and not to the overall dynamics in the $n\pi^*$ state or the ground state, which leads to the fragmentation and may be much longer. The problem becomes more complex upon complexation, i.e. the protonated thymine exhibits a broad vibrational bands spectrum whereas its protonated dimer shows structured and well resolved vibrational progressions, which means that relaxation in the dimer is slower than in the monomer.²¹ A similar effect is observed in the complex formed by cytosine and Ag^+ .²²

Why is the excited lifetime so much tautomer dependant is not a simple problem and in this paper we show that most of the excited state lifetimes of the protonated pyrimidines are extremely short and some general correlations with structural and energetic properties such as $\pi\pi^*/n\pi^*$ energy gap are explored to shed some light into this puzzling problem.

2. Methodology

2.1. Experimental

The experimental setup in Marseille has been described previously.²³ It consists of an electrospray ion source (ESI), a cryogenically cooled quadrupole-ion-trap (QIT) and a time-of-flight mass spectrometer (TOF-Mass). The protonated ions produced in the ESI source are guided by a couple of electrostatic lenses to the Paul trap (Jordan TOF, Inc.). The ions are cooled in the cold Paul trap by collisions with helium buffer gas injected with a pulsed valve. The ions are thermalized at around 30 K for 60 ms before the pump UV laser is introduced to dissociate the cold ions. The fragments and remaining parent ions are extracted to the TOF spectrometer after a variable delay and detected on a microchannel plates (MCP) detector. This allows following the fragmentation dynamics from 100 ns up to a few milliseconds. The lowest temporal resolution that we can achieve (100 ns) is due to the rise time of the high voltage pulse extracting the ions. The UV spectrum is obtained by scanning the laser frequency while recording the fragmentation signal. For experiments with nanosecond lasers,

the UV laser is an OPO laser (EKSPLA model-NT342B) with a spectral resolution of 10 cm^{-1} , a 10 Hz repetition rate, and a minimum scanning step of 0.02 nm. The unfocused laser is shaped to a 2 mm^2 spot in the trap, corresponding to a power of c.a. 5 mW.

Picosecond pump/probe experiments²⁴ have been performed in the CLUPS in Orsay using 2 picosecond OPA lasers (Ekspla-PG411 pumped by a mode-locked Nd:YAG laser Ekspla-SL300)). The setup is the same as the one in Marseille. The picosecond time resolved spectroscopy is recorded by delaying the probe beam (355 nm) with a motorized optical delay line with 6.6 ps time step. It should be pointed out that the interpretation of the pump/probe signal observed through photo-fragmentation signals is not straightforward. As the probe photon cannot doubly ionize the protonated molecule, the probe photon induces a transition $S_n \leftarrow S_1$. This S_n state ends up to internal conversion leading to the hot ground state having the energy of the pump and the probe photon. If after internal conversion the ground state dynamics leads to only one fragmentation channel, the excited state lifetime cannot be measured by monitoring the fragment signal. Indeed all the ions excited in S_1 have enough energy to dissociate and the addition of the probe photon does not change the fragmentation yield. To see an effect of the probe photon, one needs at least two fragments and a change of the branching ratio upon addition of the probe photon. This can lead to very complex temporal behavior as previously discussed in great detail in the case of tryptophan.²⁵

It should be noticed that faster processes occurring in the fs range cannot be evidenced with the picosecond laser system. The very short lifetimes are obtained from the line profile broadening. This measurement is possible on molecular systems which do not have very low frequency vibrational progressions as can be found in floppy molecules (amino acid). The pyrimidines are quite rigid and the lowest vibrational mode frequency is typically 150 cm^{-1} . What is measured in this case is the lifetime of the initially excited state in the Franck-Condon window, in other words the time for the wave packet to leave the near planar Franck-Condon geometry of the $\pi\pi^*$ state. It does not give information as to where the wave packet moves, either to a bent geometry of the same initially prepared state or to another electronic state ($n\pi^*$ singlet, triplet or S_0).

For an excited state lifetime in a medium range (1ps/500fs), the lifetime estimated from the bandwidth corresponds to a lower limit of the real value due to the limited spectral resolution. This method gives only an estimate of the lifetime.

2.2 Calculations

Ab initio calculations have been performed with the TURBOMOLE program package (v6.6),²⁶ making use of the resolution-of-the-identity (RI) approximation for the evaluation of the electron-repulsion integrals.²⁷ The equilibrium geometry in S_0 was determined at the MP2 level of theory. To see if there is a simple correlation between the $n\pi^*$ and $\pi\pi^*$ energy gap in the Franck-Condon region and the excited state lifetime, vertical and adiabatic excitation energies to the lowest excited singlet states with the Cs symmetry constraint were determined at the RI-CC2 level.²⁸ Calculations were performed with the cc-pVDZ basis set.²⁹ This method has proved to be suitable to simulate the spectra of the five DNA/RNA bases as well as other aromatic systems.¹⁹

3. Results

3.1. Photo-fragmentation mass spectra

All the non-substituted protonated DAz (1,2-DAz = pyridazine, 1,3-DAz = pyrimidine and 1,4-DAz = pyrazine) lose HCN while protonated pyridine loses H_2 . In this latter case, the loss of H_2 has been explained by the migration of the proton from the nitrogen atom to the nearby carbon atom through a barrier of ~ 3.1 eV and subsequent elimination of H_2 , which requires only ~ 3.8 eV.³⁰ This process requires much less energy than the energy available in the system after internal conversion and thus one expects fast fragmentation. The fragmentation time can be measured by changing the delay between the fragmentation laser and the extraction of the fragment ions from the trap: in these molecules the fragmentation time is less than 100 ns (experimental time resolution of the ion extraction from the QIT).

The photofragmentation channel of non-substituted protonated ($DAzH^+$) is the same as the one observed through Collision Induced Dissociation, i.e. loss of HCN. This channel has been recently characterized through experimental and ab-initio calculations.³¹ For the 1,2-, 1,3- and 1,4- $DAzH^+$, the reaction starts by proton transfer from the nitrogen atom to the nearby carbon atom through a barrier between c.a. 70 and 90 kcal/mol (3 and 3.9 eV), which is the highest barrier along the dissociation path. The energy of the final fragments is around 70 kcal/mol (3 eV), and the energy available in the optical excitation (4.4 eV) is higher than any barrier in the reaction path so that the reaction is energetically allowed after internal conversion. The fragmentation products observed for protonated cytosine, thymine and uracil (CH^+ , TH^+ and UH^+) are the same as those observed in collision induced dissociation or in infrared multi-photon dissociation experiments, i.e. NH_3 , H_2O and $HNCO$, which means that

very likely these fragments come from dissociation in the ground state following IC after electronic excitation.

3.2. Photo-fragmentation spectra.

The photofragmentation spectra of substituted and non-substituted 1,2-, 1,3- and 1,4-DAzH⁺ are presented in comparison with the photofragmentation spectrum of protonated pyridine (PyrH⁺) in Figure 1 (the photofragmentation spectra of protonated DNA bases, CH⁺, TH⁺ and UH⁺ have been presented in a previous publication).¹⁹ PyrH⁺, TH⁺ and 1,2-; 1,3-; 1,4-DAzH⁺ show only one tautomer while UH⁺ and CH⁺ have two. The electronic transition origins are all in the spectral region of 280 - 250 nm (4.5 - 5.0 eV) except for the tautomers containing a carbonyl group (CH⁺ and UH⁺ in their keto form) which are red shifted to 320 – 300 nm (3.9- 4.1 eV) due to the additional stabilization of the ring as a consequence of the conjugation with the π orbital of the C=O bond. The vertical lines in the spectra show the position of the 0-0 transition for the corresponding neutral species.

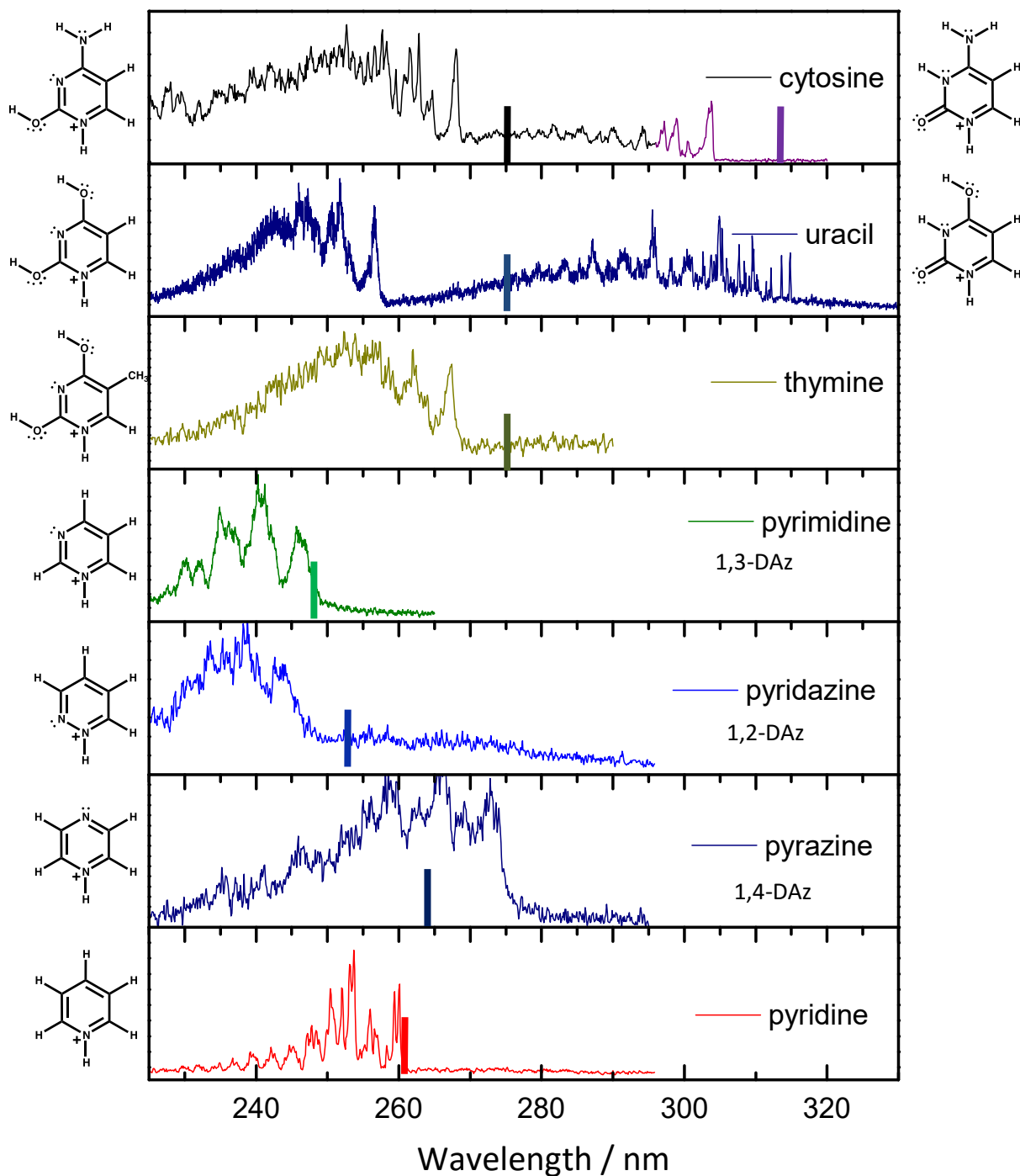


Fig. 1: Photofragmentation spectra of protonated DNA/RNA pyrimidine bases, 1,2-; 1,3- and 1,4- protonated diazine and protonated pyridine. The solid vertical lines indicate the 0-0 transitions of the neutral molecules.

Among these molecules, only one tautomer of UH^+ , assigned to the enol-keto tautomer from calculation and from hole-burning spectroscopy,^{19,32} exhibits well resolved narrow vibrational bands, while the others present broad bands as compared to the spectral resolution of the experiment. As in our previous work, the excited state lifetimes (τ) were estimated from

the relationship with the Lorentzian bandwidths (FWHM) given by the uncertainty principle ($\tau(s) = 5.3 \times 10^{-12} / \text{FWHM} (\text{cm}^{-1})$) and they are reported in Table 1. All the spectra were fitted by Voigt profiles to extract the Lorentzian bandwidths. In the case of PyrH^+ , we found a Lorentzian width of $25 \pm 10 \text{ cm}^{-1}$, which implies an excited state lifetime around $200 \pm 50 \text{ fs}$ (Figure 2). We have tested that this broadening is not due to a wide rotational envelope. Using a very pessimistic value of 100 K for the rotational temperature, ca. more than twice the estimated temperature of the ions in the cooled trap and *ab initio* calculated rotational constants, the rotational spectrum has been simulated using the Pgopher program,³³ leading to a rotational envelope convoluted by the laser (10 cm^{-1}) of 15 cm^{-1} .

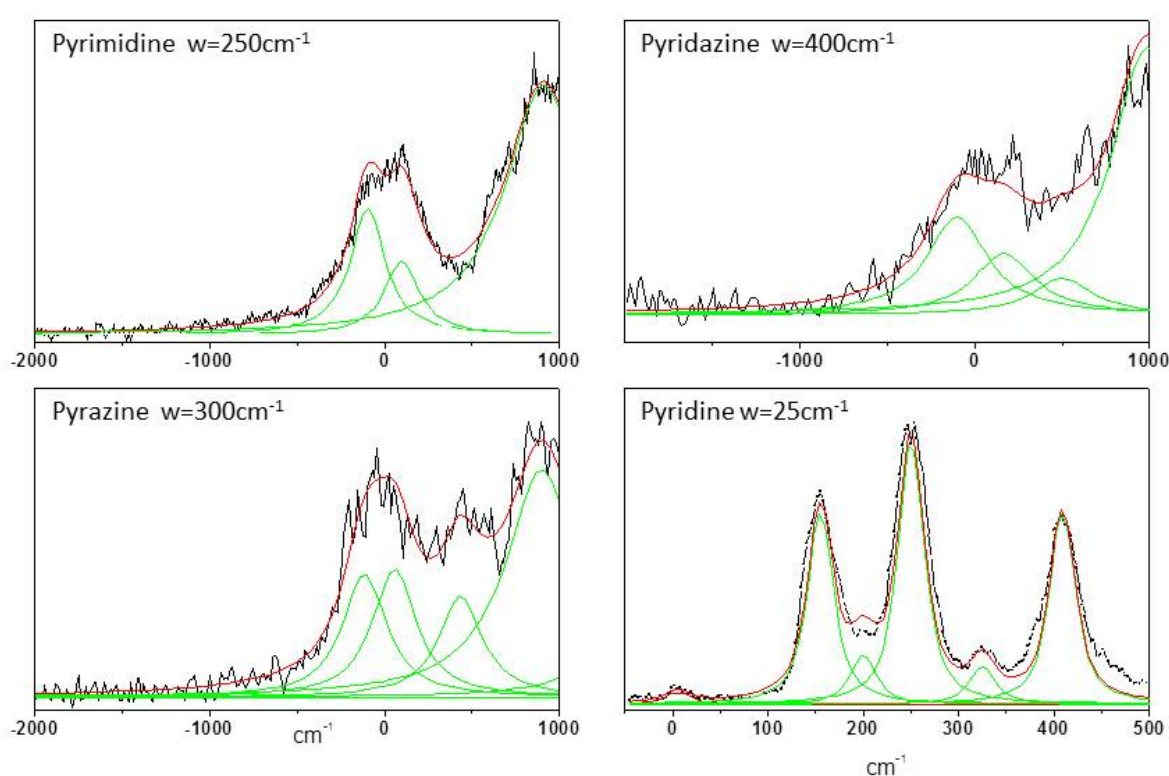


Fig. 2: Fit of the experimental spectra near the band origin with a superposition of Voigt profiles. The Gaussian width was 15 cm^{-1} and accounted for the spectral band width of the laser and the rotational contour. The Lorentzian FWHM (w) in cm^{-1} determines the excited state lifetime according to the uncertainty principle. Note the change in the x scale between Pyridine and the diazines.

3.3. Picosecond pump/probe time evolution

3.3.1. Protonated azone and diazines

For these systems, no picosecond pump-probe signal was observed, independently of the pump and probe wavelengths used. The absence of pump/probe signal is expected in different cases:

- i) The excited state may have a very short lifetime (fs) as compared to the temporal resolution of the lasers.
- ii) If only one fragment is produced and the absorption of a probe photon only increases the internal energy but not the fragmentation yield, then only the reaction rate changes. The experiment, which is detecting the fragmentation at long times, is not sensitive to the rate.³⁴

For protonated pyridine and the protonated diazine molecules in which a single fragment is observed the probe photon can only induce an acceleration of the fragmentation rate, but since the fragmentation rate is already faster than our experimental resolution (100 ns), this acceleration cannot be observed.

3.3.2. Protonated pyrimidine DNA/RNA bases

For the protonated pyrimidine DNA/RNA bases, several fragments are observed, which makes the pump/probe experiments feasible whenever the excited state lifetime is longer than the laser temporal resolution. Very short lifetimes (< 1 ps) are estimated from line broadening for most of the protonated DNA/RNA bases¹⁴ with the exception of the uracil enol-keto tautomer (see Table 1).

In the pump/probe experiment, the 2-color signal is observed as long as the fragmentation branching ratio is changing. The time evolution recorded on a specific fragmentation channel reflects the time during which the system can absorb a second photon. By choosing a probe wavelength to the red of the band origin (typically in the visible or at 355 nm), we ensure that the 2-color signal is only related to the evolution of the population in the excited state potential energy surface and not in the ground state reached after IC. In a first approximation, a mono exponential decay function observed in the transient signal is assigned to the excited state lifetime of the locally excited $\pi\pi^*$ state. However, complex transient signals can be recorded if the initially prepared population decays into a manifold of lower excited states (such as charge transfer states).³⁵

The pump/probe signal of the enol-keto tautomer of UH^+ recorded on the 0-0 transition (314.15 nm) with the probe at 355 nm is shown in Figure 3. The signal is well fitted with a mono exponential decay of 2 ns, which is consistent with the observed well-resolved vibrational spectrum. The lifetime is decreasing slowly and monotonically as the vibrational energy increases.

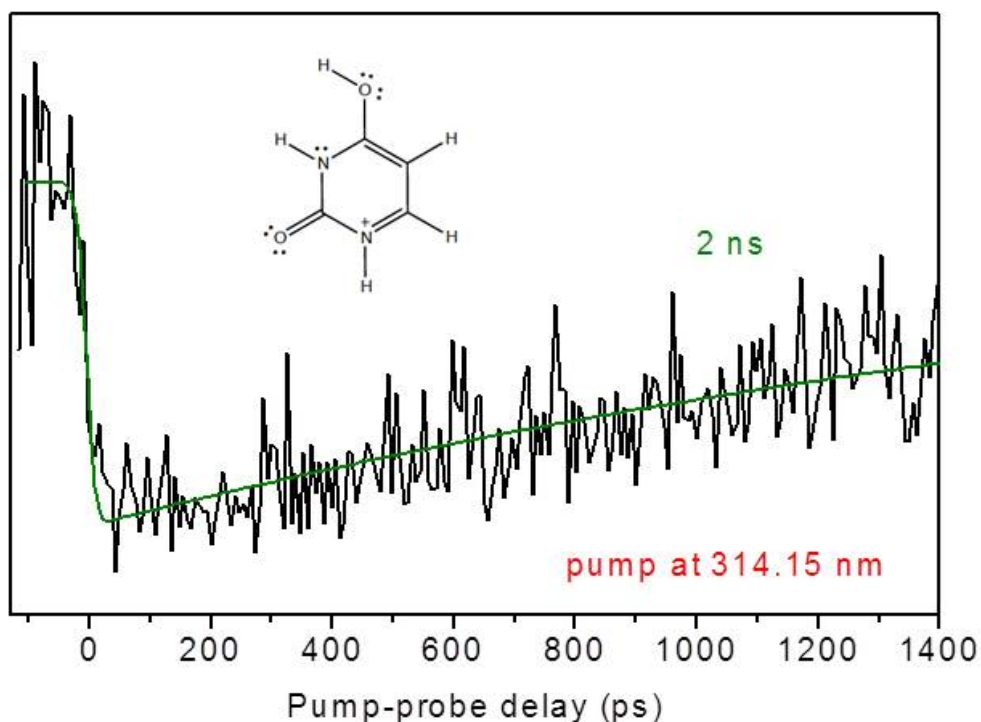


Fig. 3: Picosecond pump-probe signal of keto-enol UH^+ (black) detected on the m/z 71 fragment. The pump wavelength is set at 314.15 nm i.e. on the transition origin, and the probe wavelength is set at 355 nm. The green line is the mono exponential fitting function with a time constant of 2 ns.

4. Discussion

4.1. Calculations and tautomer assignment

The results of the calculations are summarized in Table 1. In the ground state, all the molecules have a C_s symmetry (C_{2v} for PyrH^+ and $1,4\text{-DAzH}^+$), thus the $\pi\pi^*$ (A') and the $n\pi^*$ (A'') states can be easily identified. The excited state adiabatic transition energies have been calculated at the RI-CC2 level in planar C_s symmetry since the Franck-Condon window is close to a planar structure. We have already shown in previous studies that the CC2 method provides fairly good agreement with the experimental values (within ± 0.05 eV) when the difference in zero point energy is taken into account.^{19,36} Without this correction, calculated transition energies are overestimated by c.a. 0.15 eV. As can be seen in Table 1, the error made for the DNA/RNA bases is indeed around 0.15 eV, which allows confident assignment of their tautomeric forms. The situation is however quite different for the diazine and pyridine molecules. In these cases, the calculated $\pi\pi^*$ transitions are on average 0.3 eV to the blue of the experimental transition, which is twice the expected error. It should be stressed here that

these molecules neither have tautomers nor different conformations. The discrepancy between calculated and experimental $\pi\pi^*$ transitions therefore suggests that the C_s symmetry is lost in the excited state.

Table 1: Experimental and adiabatic (CC2/cc-pVDZ) transition energies of the protonated molecules in C_s symmetry. Energies are in eV and lifetimes are in fs.

Molecules	Tautomer	$\pi\pi^*$ 0_0^0 exp	$\pi\pi^*$ C_s calc	ΔE (calc-exp)	ΔE^{calc} ($n\pi^* - \pi\pi^*$)	Lifetimes exp
Cytosine CH^+	Enol-amino	4.63	4.75	0.12	+ 0.39	100
	Keto-amino	4.08	4.17	0.09	- 0.38 ^(a)	130
Uracil UH^+	Enol-enol	4.83	5.00	0.17	+ 0.11	40
	Enol-keto	3.9	3.85	- 0.05	- 0.48 ^(a)	2×10^6
Thymine TH^+	Enol-enol	4.64	4.83	0.19	+ 0.28	58
Pyridazine 1,2-DAzH ⁺		5.08	5.42	0.28	- 1.10	13
Pyrimidine 1,3-DAzH ⁺		5.02	5.3	0.34	- 1.76	21
Pyrazine 1,4-DAzH ⁺		4.54	4.86	0.32	- 1.25	18
Pyridine PyrH ⁺		4.77	5.08	0.31	na	220

^(a) Lone pair orbital of the carbonyl oxygen atom

4.2. $\pi\pi^*$ / $n\pi^*$ state ordering and electronic configuration of the $n\pi^*$ state

The energy differences between the calculated $n\pi^*$ and $\pi\pi^*$ states ΔE^{calc} ($n\pi^* - \pi\pi^*$) are reported in Table 1 for all the molecules except for PyridineH⁺, which does not have a lone pair orbital. These differences are compared to the excited state lifetimes obtained from the vibronic line broadening and the pump/probe experiment. For protonated diazines, the $n_N\pi^*$ (nitrogen lone pair orbital) is clearly well below the locally excited $\pi\pi^*$ state, and the excited state lifetime is shorter than 50 fs. However, for the DNA/RNA bases, it can be readily deduced that no correlation can be drawn between the ordering of the $n\pi^*/\pi\pi^*$ states and the shortening of the excited state lifetime. Indeed, both keto-amino tautomer of CH^+ and enol-keto tautomer of UH^+ have $n_O\pi^*$ state below the locally excited state, but the lifetimes are drastically different. Therefore, the usual mechanism of $\pi\pi^* \rightarrow n\pi^*$ followed by $n\pi^* \rightarrow S_0$ does not necessarily hold for these protonated molecules.

Depending on the tautomeric form of the DNA/RNA bases, the electronic configuration of the $n\pi^*$ charge transfer state can be different. While most of the molecules studied have a lone pair orbital on the nitrogen atom, CH^+ in keto-amino form and UH^+ in enol-keto form have a $n_O\pi^*$ state, with the lone pair orbital on the carbonyl oxygen. In the enol-keto form, the oxygen lone pair is involved in the aromaticity and the delocalization of

the electrons can be extended to the carbonyl group at variance with enol-enol form. Thus we can explain the red shift of the enol-keto form with respect to the enol-enol form. It is worth mentioning that these two molecules have the longest excited state lifetimes along with pyridineH⁺, which does not have n π^* state. Therefore, it seems that the condition of a free lone pair on N involved in the ring is necessary for a short lived excited state with the exception of keto-amino tautomer of CH⁺ that will be discussed below.

4.3. Comparison with neutral molecules

Table 2 shows a comparison, when data are available, of the $\pi\pi^*$ and $n\pi^*$ states energies, for neutral and protonated molecules of the same tautomeric form. The origin of the $\pi\pi^* \leftarrow S_0$ transition for the protonated molecules are very close to those of the corresponding neutral molecules, with a small blue shift (0.02 – 0.18 eV) upon protonation, except for pyrazine 1,4-DAZH⁺, which shows a moderate red shift (-0.15 eV). This weak variation of the 0-0 transition indicates that the $\pi\pi^*$ state is only weakly perturbed by the addition of the proton. On the other hand, the perturbation on the $n\pi^*$ states is larger, as revealed by the changes in the energy gap ΔE^{calc} ($n\pi^* - \pi\pi^*$) between protonated and neutral forms. In the case of uracil and thymine, the protonation changes the tautomeric form and the electronic configuration of the $n\pi^*$ state. For instance, in the case of TH⁺, the molecule adopts an enol-enol conformation with the lone pair orbital localized on the N atom while in neutral thymine, a keto-keto tautomer is found with the lone pair orbital on the O atom. In these cases, the comparison between neutral and protonated molecules becomes meaningless within the discussion of this work.

Table 2: Comparison of the electronic transition energy in protonated and neutral molecules for the same tautomeric forms. Values for neutral cytosine are from ref^{37,38}, for diazine molecules from ref⁵⁻⁷. Experimental 0₀⁰ transitions and calculated energy differences ΔE^{calc} ($n\pi^* - \pi\pi^*$) are in eV.

Molecule	$\pi\pi^* 0_0^0$ exp		ΔE^{calc} ($n\pi^* - \pi\pi^*$)	
	Proton	Neutral	Proton	Neutral
Cytosine				
Enol-amino	4.63	4.50	+ 0.39	+ 0.01
Keto-amino	4.08	3.95	- 0.38	+ 0.06
Pyridazine	5.08	4.90	- 1.10	- 1.60
Pyrimidine	5.02	5.00	- 1.76	- 1.15
Pyrazine	4.54	4.69	- 1.25	- 0.86
Pyridine	4.77	4.75		- 0.44

The discussion is separated into sub-groups of molecules according to their similarities.

4.3.1. Pyridine

The photofragmentation spectrum recorded here is similar to the spectrum previously published by Hansen *et al.*³⁰ Here, the structure of each vibrational band due to the activity of out-of-plane modes (particularly nitrogen pyramidalization) is well resolved, which implies that the excited state is non planar. In the spectrum, there is a weak band at 261 nm, which is not a hot band as shown by the variation of the signal with the ion trap temperature (see Figure 2 and 1 SI), but the band origin.

In a previous work,³⁹ it was suggested that the fast deactivation pathway of the $\pi\pi^*$ state of neutral Pyr might occur through a ring-closing and is assisted by a conical intersection with the electronic surface of a prefulvene-like intermediate species. After passing through the conical intersection the molecule re-aromatizes in a barrierless process to repopulate the S_0 state, providing an alternative photochemical route.

The excited state lifetimes of the $\pi\pi^*$ of Pyr and PyrH^+ in solution⁸ with protic and aprotic solvents were determined to be the same (2.2 ps) indicating that the $n\pi^*$ state is not involved in the main deactivation pathway of the $\pi\pi^*$ state and the photochemical mechanisms described above was invoked to rationalize these results. From the bandwidth of the photofragmentation spectrum of PyrH^+ , we obtain an excited state lifetime of around 0.2 ps, which is shorter than the liquid phase value. This can be understood if this short lifetime is due to the strong out of plane deformation of the $\pi\pi^*$, as suggested in ref³⁰, the solvent can inhibit and/or slow down these dynamics.

4.3.2. Diazines

The photofragmentation spectra of the three DAzH^+ present very broad vibrational bands suggesting very short excited state lifetimes within a few tens of fs as shown in Table 1. In the DAzH^+ , the two lowest excited states have $n\pi^*$ character while the $\pi\pi^*$ state is the third excited state. Excited state optimization without symmetry restriction of these states shows that the first $n\pi^*$ state stays planar upon optimization, the second $n\pi^*$ also stays planar for 1,3- DAzH^+ and 1,2- DAzH^+ but not for 1,4- DAzH^+ . The striking result is that for the three diazines, the $\pi\pi^*$ optimization leads to out of plane deformations and a barrier free conical intersection with the second $n\pi^*$ state (point at which the CC2 calculation cannot converge). One can therefore presume that the short lifetime is due to the usual paradigm, a fast relaxation from the $\pi\pi^*$ to a lower $n\pi^*$ state as in neutral DAz .^{9,10}

4.3.3. DNA/RNA bases

For the three neutral pyrimidine DNA/RNA bases, two different mechanisms have been suggested to be responsible for the fast IC to the ground state. One of them is the direct mechanism, a conical intersection (CI) between the $\pi\pi^*$ and the S_0 state. The other one is an indirect mechanism that involves CI from the $\pi\pi^*$ to the $n_O\pi^*$ state and a subsequent CI from the $n\pi^*$ to the S_0 state. Several CIs have been located for each molecule, and all of them are characterized by strongly bent geometries, involving distortions of the rings or pyramidalization of the NH_2 group.

Non-adiabatic dynamics simulations in general find that the indirect mechanisms via two CIs are responsible for the major deactivation route. However, it must be noted that these calculations are performed at excitation energies close to the vertical excitation or to 266 nm (a common excitation wavelength for femtosecond pump-probe experiments), well above the adiabatic transition at which the excited state lifetimes were determined in this work, thus different regions of the potential energy surface are sampled. Moreover, works dealing with the calculations of the potential energy surfaces and the location of the CIs suggest that most likely the direct mechanism takes place at energies near the minimum of the $\pi\pi^*$ state surface since the CI between this state and S_0 is the lowest one.^{38,40}

Thymine: The photofragmentation spectrum of TH^+ shows a single isomer, assigned by calculations to the enol-enol tautomer with an excited state lifetime in the order of a 60 fs. The gas phase spectrum of the keto-keto form of neutral thymine is a very broad unstructured band with the origin around 4.50 eV.⁴¹ The lack of structure in the spectrum is assigned to a very short excited state lifetime due to an ultrafast non-radiative deactivation process. A CI between the $\pi\pi^*$ state and the S_0 state has been located, which is accessible in a barrierless manner⁴⁰ or via a small energy barrier⁴² from the minimum of the $\pi\pi^*$ state, providing a direct pathway for the fast deactivation of the excited state. The other mechanism invokes a first CI between the $\pi\pi^*$ state and the $n_O\pi^*$ state followed by a second CI between the $n_O\pi^*$ and the S_0 states.⁴³

For the enol-enol protonated tautomer in which the n_O orbitals are unavailable, the only low lying $n\pi^*$ state is built on the n orbital localized on the N atom ($n_N\pi^*$) and its energy in Cs geometry is 0.28 eV above the energy of the $\pi\pi^*$ state. Therefore, a direct comparison with the second mechanism suggested for the neutral form is not possible since the low-lying

$n\pi^*$ state involved is built on the n orbital localized on an O atom. However, the excited state lifetime is still ultra-short (~ 60 fs) upon protonation. It might be an indication that the direct mechanism, i.e. CI the $\pi\pi^*$ state and S_0 , could be the most important deactivation route upon excitation near the 0-0 transition. In that case, the $n\pi^*$ state is not involved and the relative position of the states does not affect the excited state lifetime.

Uracil: The two bands in the photofragmentation spectrum of UH^+ have been assigned to two different isomers. The enol-enol tautomer 0-0 transition is located at 4.83 eV and has a very short excited state lifetime although the $n_N\pi^*$ state is 0.11 eV above the $\pi\pi^*$ state. Geometry optimization of the $\pi\pi^*$ state without symmetry constraint leads to ring deformation and large state mixing. Therefore, it is likely that the deactivation of the $\pi\pi^*$ state in enol-enol UH^+ takes place through a direct mechanisms as suggested by Delchev *et al.*¹³ for neutral uracil.

The enol-keto tautomer is red shifted with the 0-0 transition at 3.90 eV. This tautomer has the longest excited state lifetime (2 ns) among the molecules studied in this work. In this tautomer, the $n_O\pi^*$ state lies 0.48 eV below the adiabatic energy of the $\pi\pi^*$ state in the Cs optimized geometry. But, when optimizing these states without symmetry restrictions, both the S_1 ($n_O\pi^*$) and S_2 ($\pi\pi^*$) states stay planar making unlikely a CI between these two states. However, the CI could be located at higher energies and its effectiveness in the fast relaxation will depend on its relative energy with respect to the excitation energy in the Franck-Condon region. It is worth mentioning that the planar geometry of the $\pi\pi^*$ state precludes an efficient coupling with the electronic ground state. So the long excited state lifetime of enol-keto UH^+ is likely due to the absence of CI between the $\pi\pi^*$ state and either the $n\pi^*$ or the S_0 states in the Franck-Condon region.

Cytosine: two isomers (enol-amino and keto-amino) with short excited state lifetimes have been assigned for CH^+ . One can view the two tautomers as protonation in different sites of the single neutral keto-amino tautomer, which is the biologically relevant species. The $\pi\pi^*$ states for the protonated keto-amino and enol-amino tautomers (Table 2) are found at 0.13 eV and 0.68 eV higher in energy than the corresponding $\pi\pi^*$ state of the neutral keto-amino tautomer. The $n_N\pi^*$ state of protonated cytosine in its enol-amino form is 0.39 eV above the $\pi\pi^*$ state in Cs symmetry. Moreover, geometry optimization of the $\pi\pi^*$ state without Cs constraint leads to a direct internal conversion with the ground state, in agreement with the short excited state lifetime.

The excited state lifetime of the 0-0 band in the neutral keto-amino tautomer has been determined to be 40 ps from the bandwidth,⁴⁴ while there is no information for the neutral enol-amino excited state lifetime. In the case of CH^+ , both tautomers have excited state lifetimes in the order of 100 fs (Table 1), indicating that protonation induces a shortening in the excited state lifetime.

In the case of neutral keto-amino tautomer, the $n_{\text{O}}\pi^*$ state is found slightly above the $\pi\pi^*$ state by 0.06 eV (see Table 2). Ismail et al.⁴⁵ suggested that this state could be involved in the indirect mechanism. However, other studies have postulated a direct mechanism through a low $\pi\pi^*/S_0$ energy barrier.^{38,46} In the protonated keto-amino tautomer, the $n_{\text{O}}\pi^*$ is 0.38 eV below the $\pi\pi^*$ state. Optimization of the $\pi\pi^*$ state without geometry constraints leads to a CI with the $n\pi^*$ state involving rotation and pyramidalization of the NH_2 group. In this case also the short $\pi\pi^*$ lifetime can be due to the fast relaxation from the $\pi\pi^*$ to the lower $n\pi^*$ state but the coordinate is not a ring deformation as for the DAzH^+ , but through coordinates linked to the NH_2 substituent.

Finally, it should be stressed that UH^+ enol-keto form and CH^+ keto-amino form have lifetimes that vary over 4 orders of magnitude although they only differ by the functional group ($-\text{NH}_2$ or $-\text{OH}$) in position 4, but nevertheless have very similar excitation energies and energy gaps between the $\pi\pi^*$ and $n_{\text{O}}\pi^*$ states. This behavior is an evidence of the extreme sensitivity of the excited state properties upon small structural and/or chemical changes, i.e. the role of the $-\text{NH}_2$ group in the fast deactivation of CH^+ .

6. Conclusions

The photofragmentation spectra of the three protonated pyrimidine DNA/RNA bases, protonated pyridine and protonated 1,2-, 1,3- and 1,4-diazines are reported together with the excited state lifetimes estimated from the linewidths. The experimental results are complemented by *ab-initio* calculations on the ground and electronically excited states and compared with previously reported results on the corresponding neutral molecules. In general, protonation induces a shortening of the excited state lifetime as compared to the neutral molecules, while it does not affect significantly the position of the $\pi\pi^*$ states. However, depending on the protonation site, different $n\pi^*$ states can be present/absent with the lone pair orbital localized on the N or O atoms. The clear correlation that can be drawn from the present results is that if one nitrogen atom of the ring is not protonated, the excited state lifetime is very short.

Acknowledgments

This work has been conducted under the International Associated Laboratory LIA/LEMIR with financial supports of ECOS-MinCyT cooperation program (A11E02), the ANR Research Grant (ANR2010BLANC040501), FONCyT, CONICET, SeCyT-UNC and CNRS GDR EMIE. We acknowledge the use of the computing facility cluster GMPCS of the LUMAT federation (FRLUMAT 2764).

References

- 1 A. Abo-Riziq, L. Grace, E. Nir, M. Kabelac, P. Hobza and M. S. de Vries, *Proc. Natl. Acad. Sci.*, 2005, **102**, 20–23.
- 2 A. C. Rios and Y. Tor, *Isr. J. Chem.*, 2013, **53**, 469–483.
- 3 K. K. Innes, I. G. Ross and W. R. Moomaw, *J. Mol. Spectrosc.*, 1988, **132**, 492–544.
- 4 I. Yamazaki, T. Murao, K. Yoshihara, M. Fujita, K. Sushida and H. Baba, *Chem. Phys. Lett.*, 1982, **92**, 421–424.
- 5 D. B. McDonald, G. R. Fleming and S. A. Rice, *Chem. Phys.*, 1981, **60**, 335–345.
- 6 Y. Matsumoto, S. K. Kim and T. Suzuki, *J. Chem. Phys.*, 2003, **119**, 300.
- 7 A. K. Jameson and E. C. Lin, *Chem. Phys. Lett.*, 1981, **79**, 326–330.
- 8 M. Chachisvilis and A. H. Zewail, *J. Phys. Chem. A*, 1999, **103**, 7408–7418.
- 9 V. Stert, P. Farmanara and W. Radloff, *J. Chem. Phys.*, 2000, **112**, 4460.
- 10 Y.-I. Suzuki, T. Fujii, T. Horio and T. Suzuki, *J. Chem. Phys.*, 2010, **132**, 174302.
- 11 K. Kleinermanns, D. Nachtigallová and M. S. de Vries, *Int. Rev. Phys. Chem.*, 2013, **32**, 308–342.
- 12 S. Lobsiger, S. Blaser, R. K. Sinha, H.-M. Frey and S. Leutwyler, *Nat. Chem.*, 2014, **6**, 989–993.
- 13 V. B. Delchev, A. L. Sobolewski and W. Domcke, *Phys. Chem. Chem. Phys.*, 2010, **12**, 5007–5015.
- 14 S. Matsika, *J. Phys. Chem. A*, 2004, **108**, 7584–7590.

- 15 P. Carbonniere, C. Pouchan and R. Improta, *Phys. Chem. Chem. Phys.*, 2015, **17**, 11615–11626.
- 16 X. Zhang and J. M. Herbert, *J. Phys. Chem. B*, 2014, **118**, 7806–7817.
- 17 I. Cacelli, A. Ferretti and G. Prampolini, *J. Phys. Chem. A*, 2015, **119**, 5250–5259.
- 18 B. Lucas, M. Barat, J. a Fayeton, M. Perot, C. Jouvét, G. Grégoire and S. Brøndsted Nielsen, *J. Chem. Phys.*, 2008, **128**, 164302.
- 19 M. Berdakin, G. Féraud, C. Dedonder-Lardeux, C. Jouvét and G. A. Pino, *Phys. Chem. Chem. Phys.*, 2014, **16**, 10643.
- 20 S. Ø. Pedersen, C. S. Byskov, F. Turecek and S. B. Nielsen, *J. Phys. Chem. A*, 2014, **118**, 4256–4265.
- 21 G. Féraud, M. Berdakin, C. Dedonder, C. Jouvét and G. a Pino, *J. Phys. Chem. B*, 2015, **119**, 2219–2228.
- 22 M. I. Taccone, G. Féraud, M. Berdakin, C. Dedonder-Lardeux, C. Jouvét and G. A. Pino, *J. Chem. Phys.*, 2015, **143**, 041103.
- 23 I. Alata, J. Bert, M. Broquier, C. Dedonder, G. Féraud, G. Grégoire, S. Soorkia, E. Marceca and C. Jouvét, *J. Phys. Chem. A*, 2013, **117**, 4420–4427.
- 24 M. Broquier, S. Soorkia and G. Grégoire, *Phys. Chem. Chem. Phys.*, 2015, **17**, 25854–25862.
- 25 H. Kang, C. Jouvét, C. Dedonder-Lardeux, S. Martrenchard, C. Charrière, G. Grégoire, C. Desfrancois, J.-P. P. Schermann, M. Barat and J. A. Fayeton, *J. Chem. Phys.*, 2005, **122**, 084307.
- 26 R. Ahlrichs, M. Bär, M. Häser, H. Horn and C. Kölmel, *Chem. Phys. Lett.*, 1989, **162**, 165–169.
- 27 F. Weigend and M. Häser, *Theor. Chem. Accounts Theory, Comput. Model. (Theoretica Chim. Acta)*, 1997, **97**, 331–340.
- 28 A. Köhn and C. Hättig, *J. Chem. Phys.*, 2003, **119**, 5021.
- 29 C. Hättig, *Phys. Chem. Chem. Phys.*, 2005, **7**, 59.
- 30 C. S. Hansen, S. J. Blanksby, N. Chalyavi, E. J. Bieske, J. R. Reimers and A. J. Trevitt, *J. Chem. Phys.*, 2015, **142**, 014301.
- 31 Z. Wang, C. A. Cole, T. P. Snow and V. M. Bierbaum, *Astrophys. J.*, 2015, **102**, 4–11.
- 32 G. Féraud, C. Dedonder, C. Jouvét, Y. Inokuchi, T. Haino, R. Sekiya and T. Ebata, *J. Phys. Chem. Lett.*, 2014, **5**, 1236–1240.
- 33 C. M. Western, PGOPHER, a Program for Simulating Rotational, Vibrational and Electronic Structure. University of Bristol, Bristol.

- 34 G. Grégoire, H. Kang, C. Dedonder-Lardeux, C. Jouvét, C. Desfrancois, D. Onidas, V. Lepere and J. A. Fayeton, *Phys. Chem. Chem. Phys.*, 2006, **8**, 122–128.
- 35 H. Kang, C. Dedonder-Lardeux, C. Jouvét, G. Grégoire, C. Desfrancois, J.-P. Schermann, M. Barat and J. a. Fayeton, *J. Phys. Chem. A*, 2005, **109**, 2417–2420.
- 36 G. Feraud, M. Broquier, C. Dedonder, C. Jouvét, G. Gregoire and S. Soorkia, *J. Phys. Chem. A*, 2015, **119**, 5914–5924.
- 37 E. Nir, I. Hünig, K. Kleinermanns and M. S. de Vries, *Phys. Chem. Chem. Phys.*, 2003, **5**, 4780.
- 38 K. Tomić, J. Tatchen and C. M. Marian, *J. Phys. Chem. A*, 2005, **109**, 8410–8418.
- 39 A. L. Sobolewski and W. Domcke, *Chem. Phys. Lett.*, 1991, **180**, 381–386.
- 40 S. Perun, A. L. Sobolewski and W. Domcke, *J. Phys. Chem. A*, 2006, **110**, 13238–44.
- 41 B. B. Brady, L. A. Peteanu and D. H. Levy, *Chem. Phys. Lett.*, 1988, **147**, 538–543.
- 42 S. Yamazaki and T. Taketsugu, *J. Phys. Chem. A*, 2012, **116**, 491–503.
- 43 M. Barbatti, A. J. A. Aquino, J. J. Szymczak, D. Nachtigallova, P. Hobza and H. Lischka, *Proc. Natl. Acad. Sci.*, 2010, **107**, 21453–21458.
- 44 S. Lobsiger, M. A. Trachsel, H.-M. Frey and S. Leutwyler, *J. Phys. Chem. B*, 2013, **117**, 6106–15.
- 45 N. Ismail, L. Blancafort, M. Olivucci, B. Kohler and M. A. Robb, *J. Am. Chem. Soc.*, 2002, **124**, 6818–6819.
- 46 M. Merchán and L. Serrano-Andrés, *J. Am. Chem. Soc.*, 2003, **125**, 8108–8109.